nature neuroscience

SUPPLEMENTARY INFORMATION

https://doi.org/10.1038/s41593-018-0322-y

In the format provided by the authors and unedited.

Intersectional monosynaptic tracing for dissecting subtype-specific organization of GABAergic interneuron inputs

Michael J. Yetman[1], Eric Washburn[1], Jung Ho Hyun[2], Fumitaka Osakada[3,4], Yasufumi Hayano[1], Hongkui Zeng[5], Edward M. Callaway[3], Hyung-Bae Kwon[2,6] and Hiroki Taniguchi[1,7]*

[1]Development and Function of Inhibitory Neural Circuits, Max Planck Florida Institute for Neuroscience, Jupiter, FL, USA. [2]Cellular Basis of Neural Circuit Plasticity, Max Planck Florida Institute for Neuroscience, Jupiter, FL, USA. [3]Systems Neurobiology Laboratory, The Salk Institute for Biological Studies, La Jolla, CA, USA. [4]Laboratory of Cellular Pharmacology, Nagoya University, Furocho, Aichi, Japan. [5]Allen Institute for Brain Science, Seattle, WA, USA. [6]Max Planck Institute for Neurobiology, Martinstried, Germany. [7]PRESTO, Japan Science and Technology Agency, Chiyodaku, Tokyo, Japan.
*e-mail: hiroki.taniguchi@mpfi.org

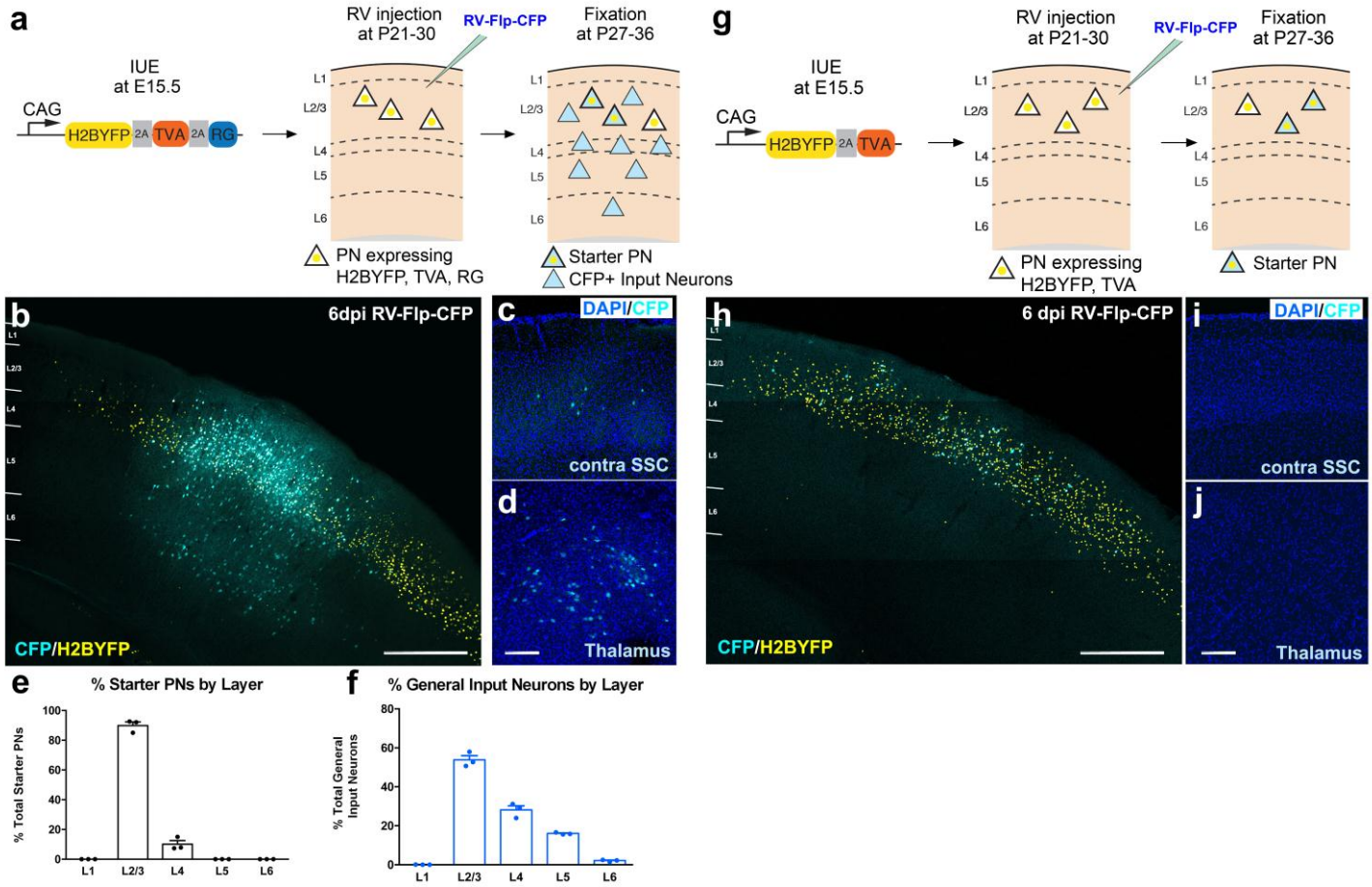

Supplementary Figure 1

Mono-trans-synaptic spread of *RV-Flp-CFP* viruses depends on expression of RG in starter PNs (Related to **Figs. 1 and 2**).
(**a**) Experimental schema for monosynaptic tracing of input neurons sending direct inputs to supragranular PNs.
(**b**) Confocal projection image merging H2BYFP (yellow) and CFP (cyan). CFP+/H2BYFP+ and CFP+/H2BYFP- represent starter PNs, and general input neurons respectively of animals prepared as shown in **a**. Scale bar, 500 µm.
(**c,d**) Confocal projection images merging DAPI (blue) and CFP (cyan) signals in the contralateral SSC (**c**) and the thalamus (**d**) of animals prepared as shown in **a**. Scale bar, 200 µm.
(**e**) Quantification of the laminar distribution of CFP+/H2BYFP+ starter PNs (**e**; L1: 0 %, L2/3: 89.9 ± 4.3 %, L4: 10.1 ± 4.3 %, L5: 0 %, L6: 0 %; 7680 cells, 3 animals) and CFP+/H2BYFP- general input neurons (**f**; L1: 0.2 ± 0.2 %, L2/3: 55.1 ± 2.9 %, L4: 28.7 ± 0.9 %, L5: 15.1 ± 1.9 %, L6: 1.0 ± 0.1 %; 23,317 cells, 3 animals)
(**g**) Experimental schema for control experiments that test dependency of RV transsynaptic spread on RG expression in starter PNs .
(**h**) Confocal projection image merging H2BYFP (yellow) and CFP (cyan). CFP+/H2BYFP+ and CFP+/H2BYFP- represent starter PNs, and general input neurons respectively of animals prepared as shown in **g**. Scale bar, 500 µm.
(**i,j**) Confocal projection images with DAPI (blue) and CFP (cyan) channels in the contralateral SSC (**i**) and the thalamus (**j**) of animals prepared as shown in **g**. Scale bar, 200 µm.
Data are presented as mean ± SEM. All experiments were repeated independently three times with similar results.

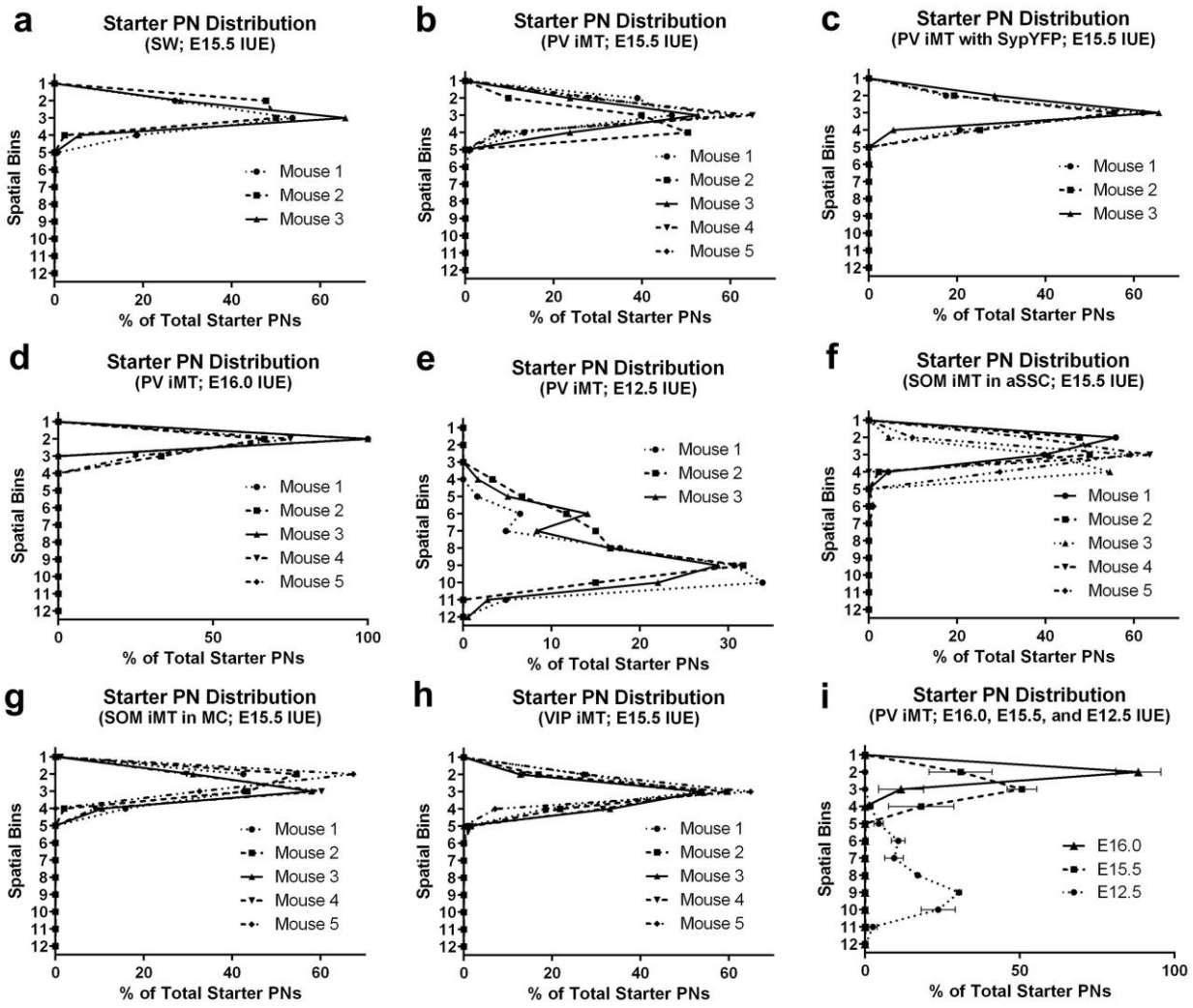

Supplementary Figure 2

Position of starter PNs from iMT within 100-µm spatial bins (Related to **Figs. 3–7**).

(**a-h**) Quantification of the spatial distribution of CFP+/H2BYFP+ or CFP+/HAH2B+ starter PNs of individual animals for iMT with control SW animals targeting supragranular PNs (IUE at E15.5)(**a**), PV-INs targeting supragranular PNs (IUE at E15.5)(**b**), PV-INs targeting supragranular PNs (SypYFP condition)(IUE at E15.5)(**c**), PV-INs targeting upper supragranular PNs (IUE at E16.0)(**d**), PV-INs targeting granular/infragranular PNs (IUE at E12.5)(**e**), SOM-INs targeting aSSC supragranular PNs (IUE at E15.5)(**f**), SOM-INs targeting MC supragranular PNs (IUE at E15.5)(**g**), and VIP-INs targeting supragranular PNs (IUE at E15.5)(**h**).
(**i**) Quantification of the spatial distribution of CFP+/H2BYFP+ or CFP+/HAH2B+ starter PNs for iMT with PV-INs targeting PNs with E16.0 (n = 5 animals), E15.5 (n = 5 animals), or E12.5 IUEs (n = 3 animals).
Data are presented as mean ± SEM.
See **Supplementary Table 2,3,5,7,9,11** for numerical values and statistics.

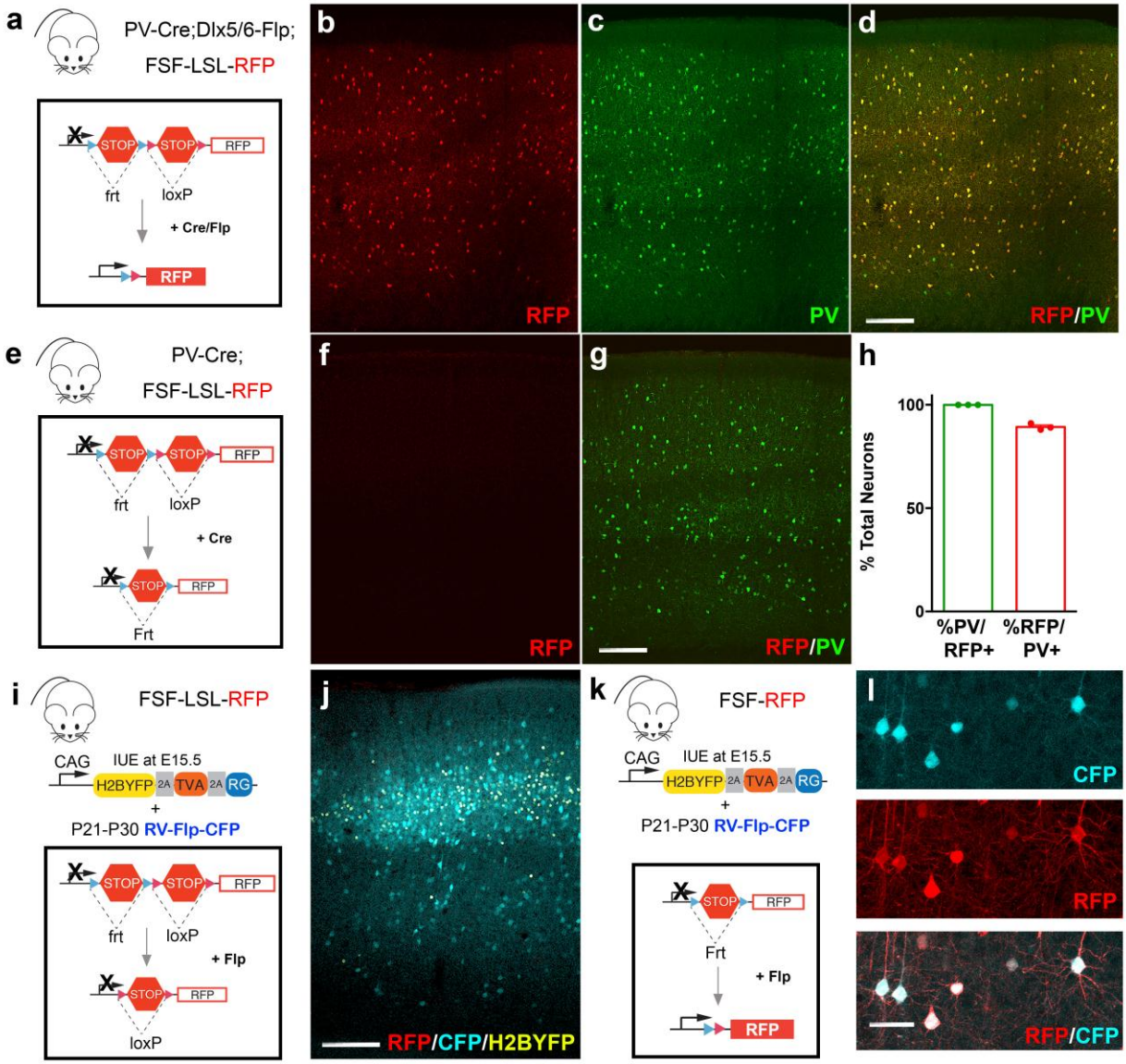

Supplementary Figure 3

RFP reporter mice are both specific and efficient. (Related to **Fig. 2**).
(**a**) Schematic showing mouse genotype (*PV-Cre;Dlx5/6-Flp;FSF-LSL-RFP*) and expected recombination at dual reporter allele.
(**b-d**) Confocal projection images of RFP (**b**), PV (**c**), and RFP/PV (**d**) signals in the same section from a *PV-Cre;Dlx5/6-Flp;FSF-LSL-RFP* mouse brain. Scale bar, 200 μm.
(**e**) Schematic showing mouse genotype (*PV-Cre;FSF-LSL-RFP*) and expected recombination at dual reporter allele.
(**f,g**) Confocal projection images taken from the same section from a *PV-Cre;FSF-LSL-RFP* mouse brain. RFP channel (**f**) and RFP/PV (**g**) images. Scale bar, 200 μm.
(**h**) Specificity and efficiency of RFP expression in *PV-Cre;Dlx5/6-Flp;FSF-LSL-RFP* mice (n = 3 animals).
(**i**) Schematic showing mouse genotype (*FSF-LSL-RFP*), genetic manipulations including IUE and RV injection, and expected recombination event at dual reporter allele.
(**j**) Confocal projection image taken from a brain section from an *FSF-LSL-RFP* mouse that underwent IUE with *pCAG-H2BYFP-2A-TVA-2A-RG* plasmids and infection with *RV-Flp-CFP* viruses. H2BYFP (yellow), CFP (cyan), and RFP (red) channels are merged. Scale bar, 200 μm.
(**k**) Schematic showing mouse genotype (*FSF-RFP*), genetic manipulations including IUE and RV injection, and expected recombination event at Flp reporter allele.
(**l**) Confocal projection images taken from a brain section from an *FSF-RFP* mouse that underwent IUE with *pCAG-H2BYFP-2A-TVA-2A-RG* plasmids and infection with *RV-Flp-CFP* viruses. CFP (cyan) and RFP (red) channels are shown. Scale bar, 50 μm.
Data are presented as mean ± SEM. All experiments were repeated independently three times with similar results.

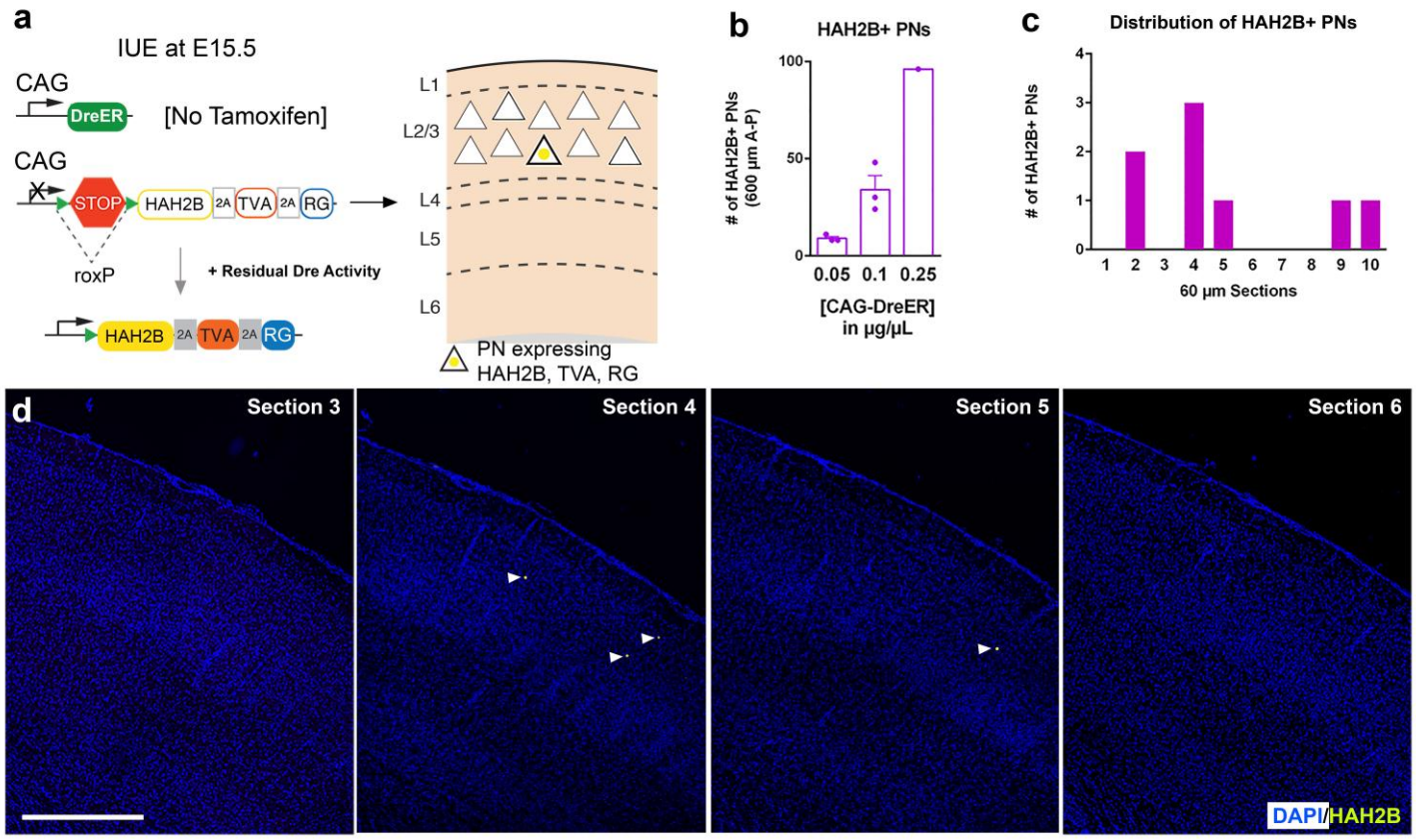

Supplementary Figure 4

Optimization for sparse expression of HAH2B, TVA, and RG in supragranular PNs (Related to **Fig. 4**).

(**a**) Experimental schema for sparse expression of HAH2B, TVA, and RG in supragranular PNs.
(**b**) Number of HAH2B+ PNs in the 500 µm A-P extent of electroporated cortical domains at distinct concentrations of *pCAG-DreER* plasmids (0.05 µg/µL: 9.0 ± 1.0, n = 3 animals; 0.1 µg/µL: 34.0 ± 7.2, n = 3 animals; 0.25 µg/µL: 96.0 ± 0.0, n = 1 animal).
(**c**) Histogram showing the number of HAH2B+ PNs in serial 60 µm sections (0.05 µg/µL *pCAG-DreER*).
(**d**) Confocal projection images taken from serial brain sections co-electroporated with *pCAG-RSR-HAH2B-2A-TVA-2A-RG* and *pCAG-DreER* (0.05 µg/µL) plasmids. DAPI (blue) and HAH2B (yellow). Arrowheads indicate HAH2B+ PNs. Scale bar, 500 µm.
Data are presented as mean ± SEM. All experiments were repeated independently three times with similar results.

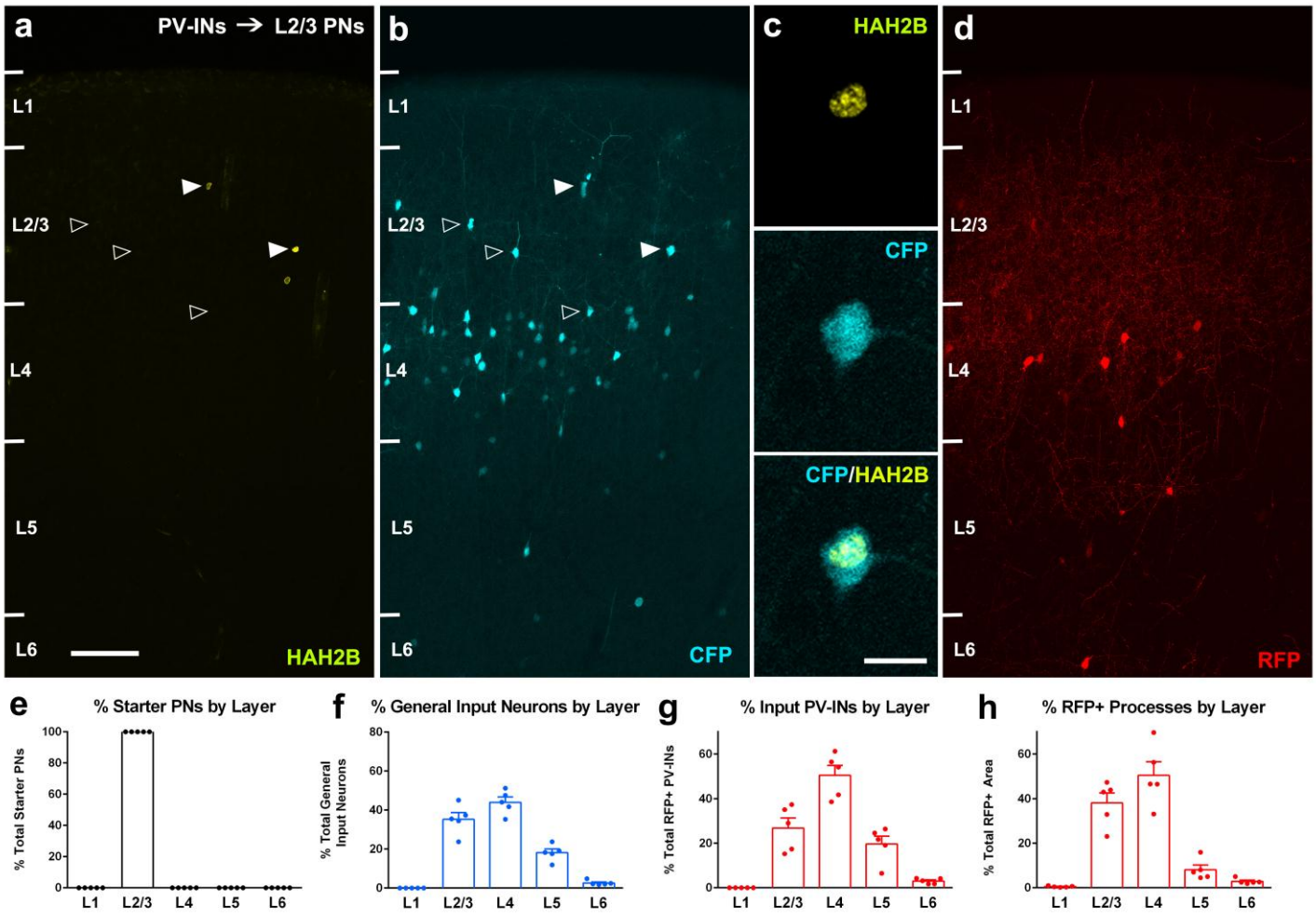

Supplementary Figure 5

Sparse L2/3 localized starter PNs exhibit similar patterns of iMT infection and innervation by PV-INs (Related to **Fig. 4**).
(**a-d**) iMT of input PV-INs innervating a sparsely labeled supragranular PNs. Confocal projection image of HAH2B (yellow) signal showing sparse expression of HAH2B in supragranular PNs (**a**) and infected CFP+ starter PNs and general input neurons (**b**). Closed and open arrowheads represent infected CFP+/HAH2B+ starter PNs and non-infected HAH2B+ PNs, respectively. Merged and single channel images from a single optical section of a CFP+/HAH2B+ starter PN indicated by closed arrowhead in **b** (**c**). Confocal projection images of RFP+ input PV-INs (red) that send inputs to CFP+/HAH2B+ PNs shown in **a-c** (**d**). Scale bars, 100 μm (**a,b,d**) and **c**) and 10 μm (**c**).
(**e-h**) Quantification of laminar distribution of CFP+/HAH2B+ starter PNs (**e**), CFP+/HAH2B- general input neurons (**f**), RFP+ input PV-INs (**g**), and RFP+ processes (**h**) (n = 5 animals).
Data are presented as mean ± SEM. All experiments were repeated independently five times with similar results.
See **Supplementary Table 4** for numerical values.

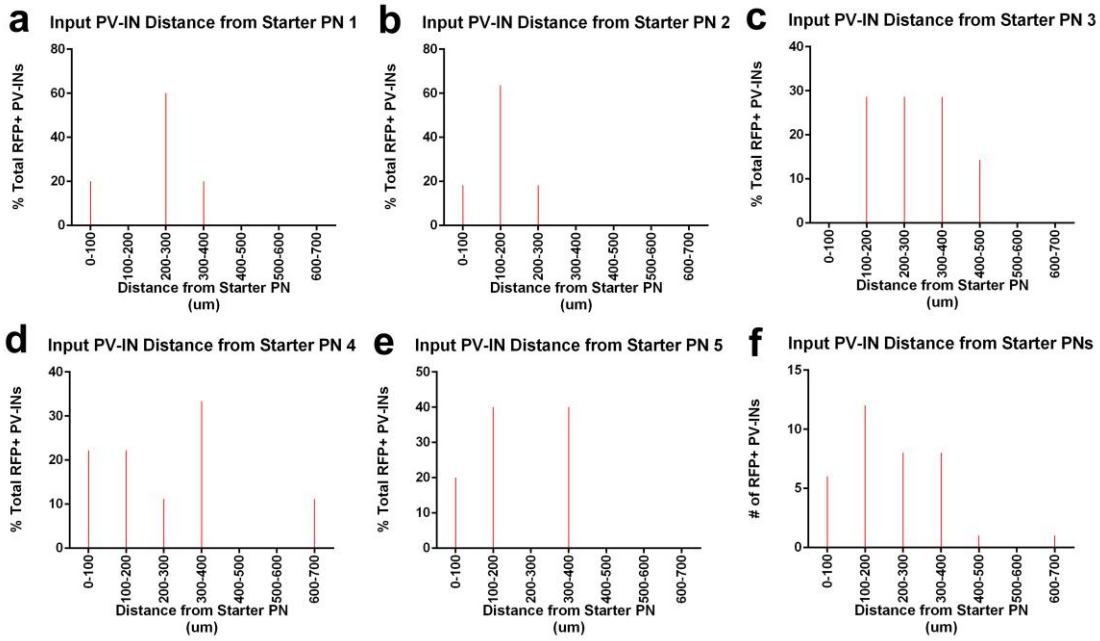

Supplementary Figure 6

Distance of input PV-INs from individual starter PNs (Related to **Fig. 4**).

(**a-f**) Histograms of the frequency of RFP+ PV-INs by absolute distance from their associated supragranular starter PNs for individual starter PNs 1-5 (**a-e**) and an aggregation of all five starter PNs (**f**).

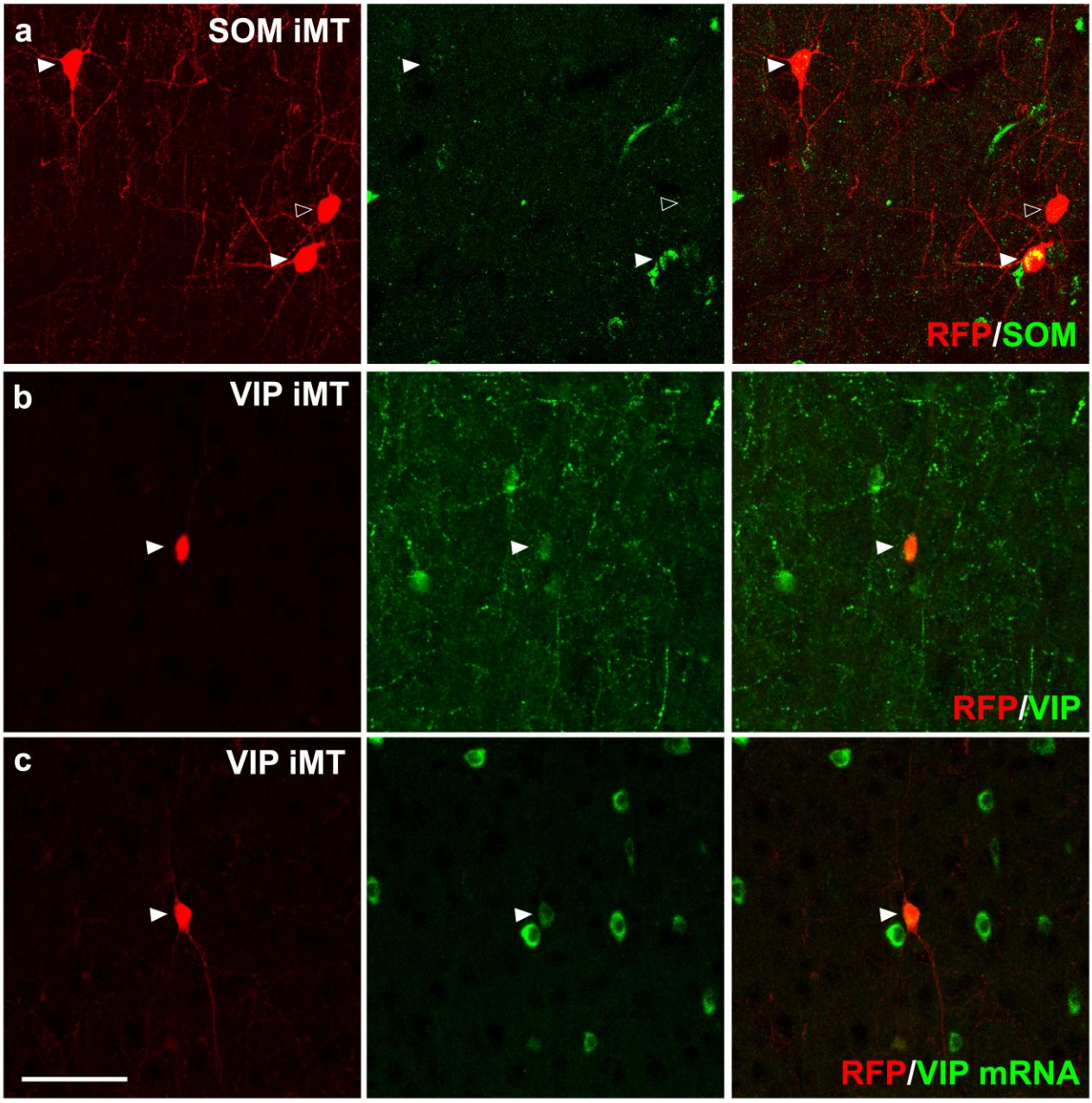

Supplementary Figure 7

Colocalization of SOM and VIP in RFP^{+} neurons from iMT (Related to **Figs. 6 and 7**).

(**a-c**) Confocal projection images from SOM iMT experiment showing RFP+/SOM+ and RFP+/SOM- neurons indicated by closed and open arrowheads, respectively. SOM is stained with anti-SOM antibodies (green).
(**b**) Confocal projection images from VIP iMT experiment showing RFP+/VIP+ neuron indicated by closed arrowhead. VIP is stained with anti-VIP antibodies (green).
(**c**) Confocal projection images from VIP iMT experiment showing RFP+/VIP+ neuron indicated by closed arrowhead. VIP is stained using anti-VIP mRNA FISH probes (green). Scale bar, 50 μm.
All experiments were repeated independently three times with similar results.

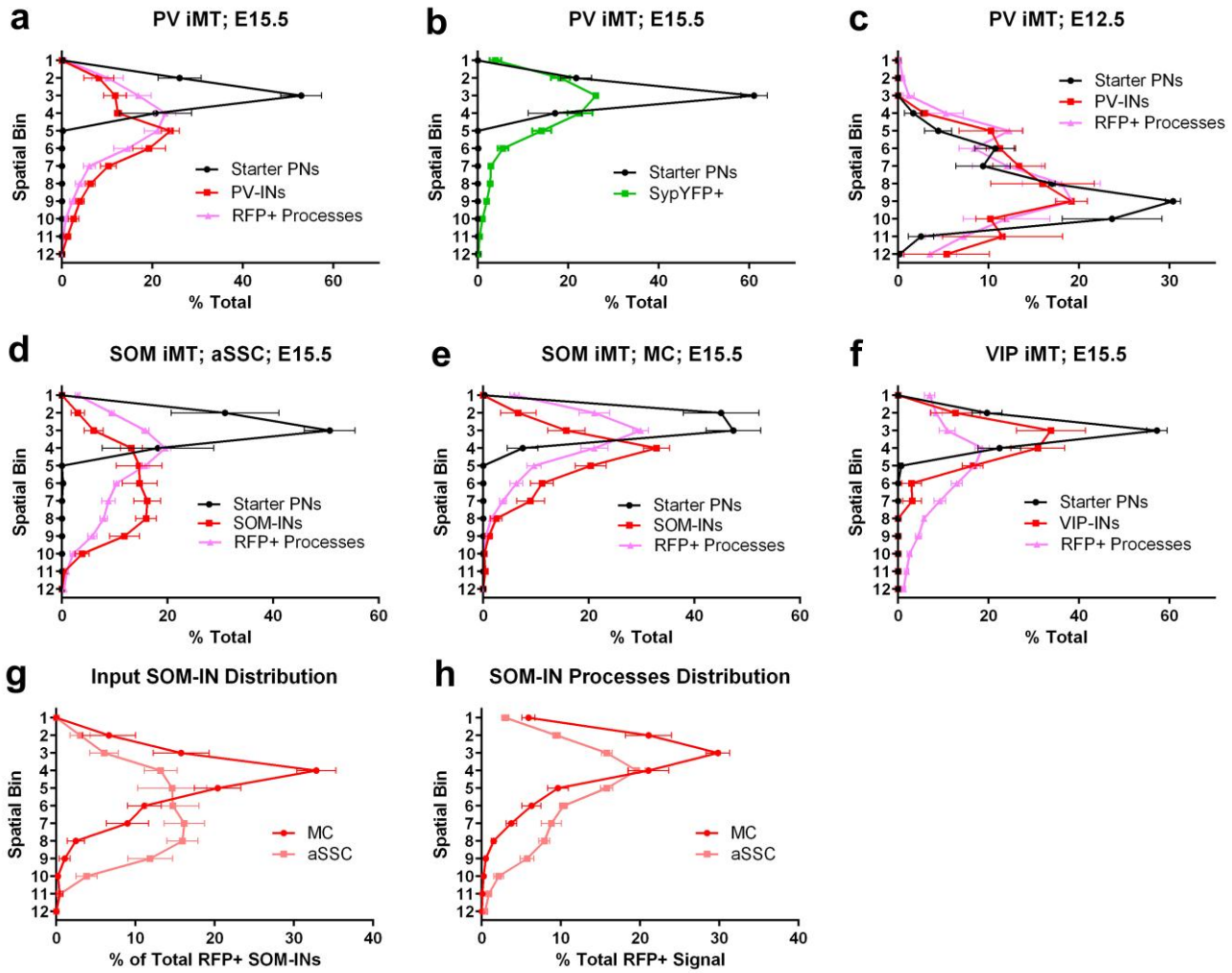

Supplementary Figure 8

Positions of starter PNs, input INs, and processes from iMT within 100-μm spatial bins (Related to **Figs. 3–7**).
(**a-f**) Quantification of the spatial distribution of starter PNs (black), RFP+ input INs (red), and RFP+/SypYFP+ signal (magenta or green) of PV-INs targeting supragranular PNs (IUE at E15.5)(**a**) (n = 5 animals), PV-INs targeting supragranular PNs (SypYFP condition)(IUE at E15.5)(**b**) (n = 5 animals), PV-INs targeting granular/infragranular PNs (IUE at E12.5)(**c**) (n = 3 animals), SOM-INs targeting supragranular PNs in aSSC (IUE at E15.5)(**d**) (n = 5 animals), SOM-INs targeting supragranular PNs in MC (IUE at E15.5)(**e**) (n = 5 animals), and VIP-INs targeting supragranular PNs (IUE at E15.5)(**f**) (n = 5 animals).
(**g-h**) Comparison of the quantification of the spatial distribution of RFP+ input SOM-INs (**g**) and RFP+ processes (**h**) between aSSC (peach) and MC (red) (IUE at E15.5) (n = 5 animals each).
Data are presented as mean ± SEM.
See **Supplementary Table 5,7,9,11** for numerical values.

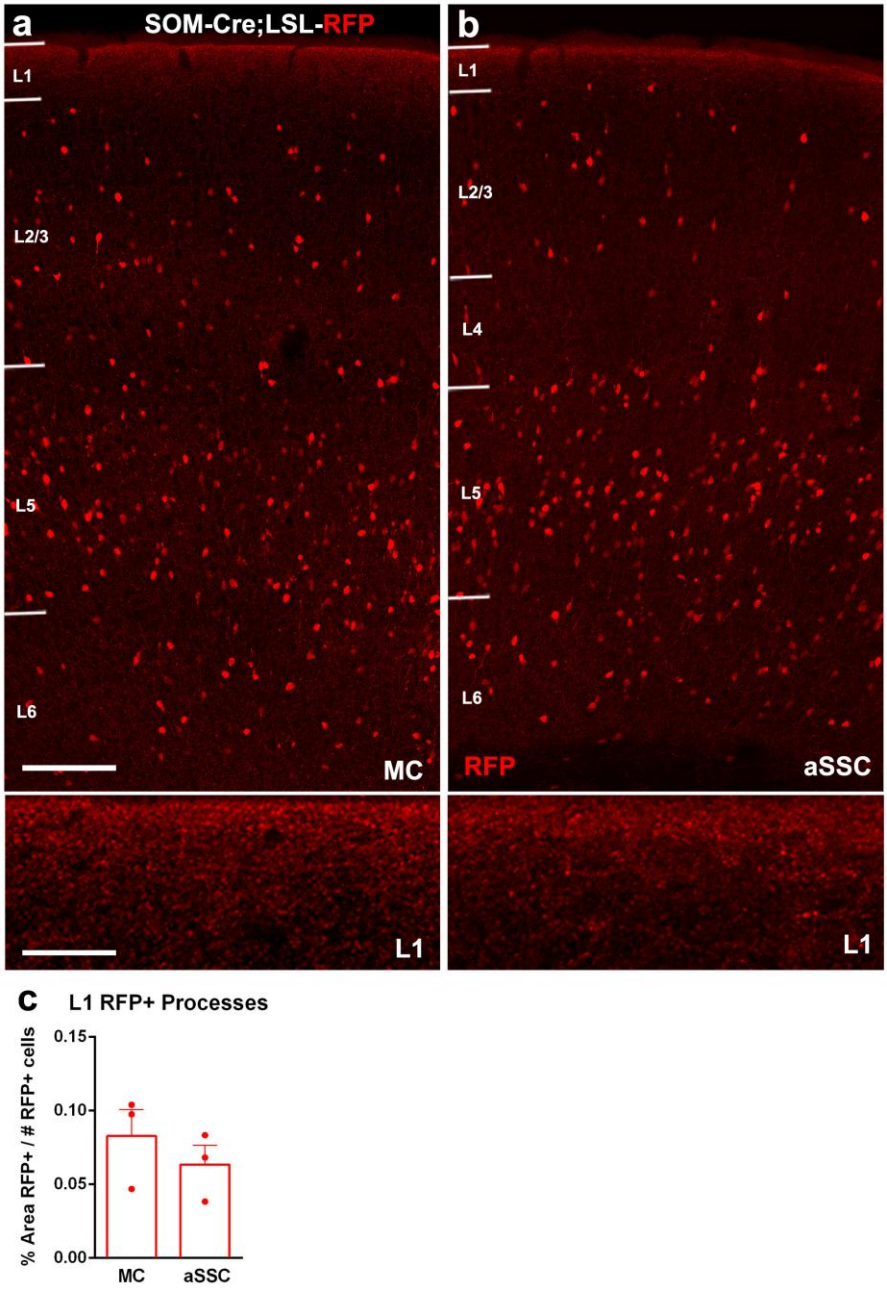

Supplementary Figure 9

Similar axonal projections to L1 by total SOM-INs in the aSSC and the MC (Related to **Fig. 6**).

(**a,b**) Confocal projection images of RFP+ SOM-INs (red) in the aSSC (**a**) and the MC (**b**) of a Cre-dependent RFP reporter mouse with *SOM-Cre* allele. Upper panels show the laminar distribution of somata and axons of all SOM-INs. Lower panels highlight L1 axons from SOM-INs. Scale bars, 200 µm (upper panels), 25 µm (lower panels).
(**c**) Area occupied by L1 RFP+ processes normalized to the number of RFP+ somata in the MC and the aSSC (n = 3 animals each). Data are presented as mean ± SEM. All experiments were repeated independently three times with similar results.
See **Supplementary Table 3** for numerical values and statistics.

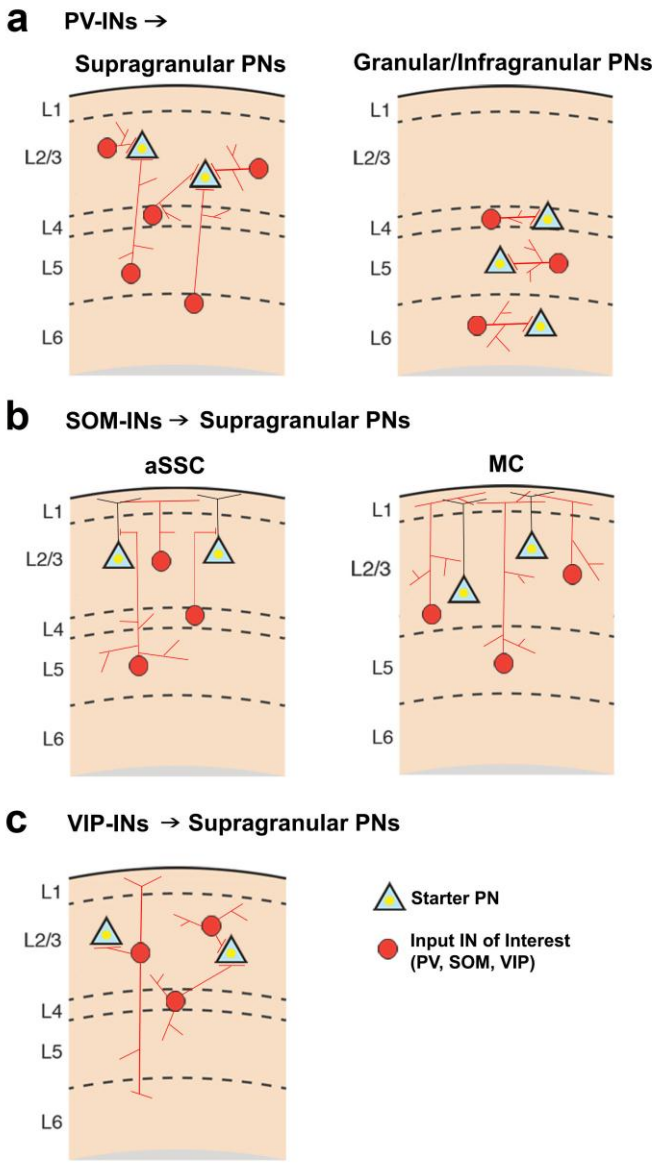

Supplementary Figure 10

Summary cartoon of iMT results.
(**a**) Summary of organization of input PV-INs that innervate supragranular or infragranular PNs in the SSC.
(**b**) Summary of organization of input SOM-INs that innervate supragranular PNs in the aSSC or the MC.
(**c**) Summary of organization of input VIP-INs that innervate supragranular PNs in the SSC.

	Genotype	Purpose in this study
Mouse Lines	*PV-Cre*	To selectively mark input PV-INs in iMT
	SOM-Cre	To selectively mark input SOM-INs in iMT
	VIP-Cre	To selectively mark input VIP-INs in iMT
	ROSA26-FSF-LSL-tdTom (FSF-LSL-RFP)	Cre/Flp-dependent dual RFP reporter line to visualize target input neurons in iMT
	ROSA26-FSF-LSL-SypYFP (FSF-LSL-SypYFP)	Cre/Flp-dependent dual SypYFP reporter line to visualize presynaptic terminals from target input neurons in iMT
	ROSA26-FSF-tdTom (FSF-RFP)	Flp-dependent RFP reporter line to test the efficiency of RV-Flp-CFP to excise stop cassette
	Name	Purpose in this study
Plasmids	*pAAV-CAG-H2BYFP-TVA-RG*	To provide PNs with starter genes
	pAAV-CAG-roxp-STOP-roxP-HAH2B-TVA-RG	To express starter genes in PNs in a Dre-dependent manner
	pAAV-CAG-DreO	To densely express starter genes from Dre-dependent plasmids in PNs for SypYFP experiments
	pAAV-CAG-DreERT2	To sparsely express starter genes from Dre-dependent plasmids in PNs using residula activity of DreER
	Name	Purpose in this study
Viruses	*EnvA-RVdG-Flp-CFP*	To selectively mark presynaptic neurons sending direct inputs to starter PNs with Flp and CFP
	EnvA-RVdG-Flp-dsRed	To selectively mark presynaptic neurons sending direct inputs to starter PNs with Flp and RFP

Supplementary Table 1. List of mouse lines, plasmids, and viruses.

PV-Cre:Ai65 *SSC*	*E15.5 IUE*	*E16.0 IUE*	*E12.5 IUE*
	CFP+/ H2BYFP+ Starter PNs	*CFP+/ HAH2B+ Starter PNs*	*CFP+/ H2BYFP+ Starter PNs*
n = 5 animals	% of 3,370 cells	% of 59 cells	% of 456 cells
Bin 1	0.2 ± 0.2	0	0
Bin 2	26.0 ± 4.8	88.3 ± 7.3	0
Bin 3	52.9 ± 4.5	11.7 ± 7.3	0
Bin 4	20.7 ± 8.0	0	1.7 ± 1.0
Bin 5	0.2 ± 0.2	0	4.4 ± 1.5
Bin 6	0	0	10.7 ± 2.3
Bin 7	0	0	9.4 ± 3.0
Bin 8	0	0	17.0 ± 0.4
Bin 9	0	0	30.4 ± 0.8
Bin 10	0	0	23.7 ± 5.5
Bin 11	0	0	2.5 ± 1.4
Bin 12	0	0	0.2 ± 0.2

Supplementary Table 2. Bin distribution of PNs in the SSC of mice that underwent E15.5, E16.0, and E12.5 IUE. Data are presented as mean ± SEM.

Comparison	*Test type*	*n*	*t/F (or X^2) values and dF*	*p-value*
Local Axons from Infragranular PV-INs– PV-INs Innervating Supra- vs. Infragranular PNs	Student's t-test, Unpaired, two-tailed	5,3	t(6) = 2.878	0.0281
Proportion of L2/3 SOM-IN Cell Bodies – MC vs. aSSC	Student's t-test, Unpaired, two-tailed	5,5	t(8) = 9.888	0.0001
Proportion of L2/3 SOM-IN Processes – MC vs. aSSC	Student's t-test, Unpaired, two-tailed	5,5	t(8) = 13.21	0.0001
L1 Axons from SOM-INs Innervating Supragranular Starter PNs- MC vs. aSSC (**Fig. 6n**)	Student's t-test, Unpaired, two-tailed	5,5	t(8) = 6.661	0.0002
L1 Axons from all SOM-INs– MC vs. aSSC (**Supplementary Fig. 6c**)	Student's t-test, Unpaired, two-tailed	3,3	t(4) = 0.8717	0.4326
Ratio of RFP+ INs to CFP+ General Input Neurons – PV vs. SOM vs. VIP	Unpaired, unmatched, one-way ANOVA	5,5,5	F(2,12) = 13.35	0.0009
Starter PN Distribution in E15.5 vs. E16.0 IUE (**Supplementary Fig. 8h, Table 10**)	Chi-square	5,5	X^2 = 114.76 dF = 7	0.0001
Starter PN Distribution in E15.5 vs. E12.5 IUE (**Supplementary Fig. 8h, Table 10**)	Chi-square	5,3	X^2 = 474.46 dF = 7	0.0001
Starter PN Distribution in E16.0 vs. E12.5 IUE (**Supplementary Fig. 8h, Table 10**)	Chi-square	5,3	X^2 = 260.0 dF = 7	0.0001

Supplementary Table 3. List of statistical tests and p-values.

PV:Ai65 *SSC (dense)*	*CFP+/ H2BYFP+ Starter PNs*	*CFP+/ H2BYFP- General Inputs*	*RFP+ Input PV-INs*	*RFP+ Processes*
n = 5 animals	% of 3,370 cells	% of 21,793 cells	% of 3,786 cells	% of total RFP
L1	0	0.1 ± 0.1	0	2.1 ± 0.3
L2/3	88.7 ± 2.9	50.9 ± 3.0	22.0 ± 3.3	39.1 ± 2.9
L4	11.3 ± 2.9	33.2 ± 2.8	32.6 ± 2.9	33.3 ± 1.4
L5	0	14.6 ± 1.1	40.6 ± 2.6	21.0 ± 1.6
L6	0	1.3 ± 0.4	4.7 ± 0.5	4.6 ± 1.0
PV:Ai65 *SSC (sparse)*	*CFP+/ HAH2B+ Starter PNs*	*CFP+/ HAH2B- General Inputs*	*RFP+ Input PV-INs*	*RFP+ Processes*
n = 5 animals	% of 59 cells	% of 913 cells	% of 336 cells	% of total RFP
L1	0	0	0	0.5 ± 0.1
L2/3	100	35.5 ± 3.4	26.8 ± 4.5	38.0 ± 4.4
L4	0	44.0 ± 2.7	50.5 ± 4.4	50.4 ± 6.1
L5	0	18.1 ± 1.9	19.7 ± 3.5	8.1 ± 2.1
L6	0	2.6 ± 0.6	3.0 ± 0.6	2.9 ± 0.6
PV:SypYFP *SSC*	*RFP+/ HAH2B+ Starter PNs*	*RFP+/ HAH2B- General Inputs*	*SypYFP+ Signal*	
n = 3 animals	*% of 2,340 cells*	*% of 21,110 cells*	*% of total YFP*	
L1	0	0.1 ± 0.1	0	
L2/3	88.7 ± 2.9	50.9 ± 3.0	22.0 ± 3.3	
L4	11.3 ± 2.9	33.2 ± 2.8	32.6 ± 2.9	
L5	0	14.6 ± 1.1	40.6 ± 2.6	
L6	0	1.3 ± 0.4	4.7 ± 0.5	

Supplementary Table 4. Laminar distribution of PV-INs that innervate supragranular PNs in the SSC. Data are presented as mean ± SEM.

PV:Ai65 *SSC*	*CFP+/ H2BYFP+ Starter PNs*	*RFP+ Input PV-INs*	*RFP+ Processes*
n = 5 animals	% of 3,370 cells	% of 3,786 cells	% of total RFP
Bin 1	0.2 ± 0.2	0	0.8 ± 0.2
Bin 2	26.0 ± 4.8	8.2 ± 3.3	10.1 ± 3.5
Bin 3	52.9 ± 4.5	11.8 ± 2.5	16.9 ± 2.8
Bin 4	20.7 ± 8.0	12.4 ± 0.8	22.9 ± 2.3
Bin 5	0.2 ± 0.2	24.0 ± 2.0	21.1 ± 2.9
Bin 6	0	19.3 ± 3.6	14.6 ± 3.1
Bin 7	0	10.3 ± 1.8	6.1 ± 1.3
Bin 8	0	6.3 ± 1.1	4.0 ± 1.0
Bin 9	0	4.0 ± 0.9	2.3 ± 0.5
Bin 10	0	2.6 ± 1.1	0.9 ± 0.3
Bin 11	0	1.2 ± 0.7	0.3 ± 0.2
Bin 12	0	0	0.08 ± 0.04
PV:SypYFP *SSC*	*RFP+/ HAH2B+ Starter PNs*	*SypYFP+ Signal*	
n = 3 animals	*% of 2,340 cells*	*% of total YFP*	
Bin 1	0	3.9 ± 1.3	
Bin 2	21.8 ± 3.4	18.3 ± 2.1	
Bin 3	61.1 ± 2.9	26.1 ± 0.3	
Bin 4	17.1 ± 5.9	22.6 ± 2.8	
Bin 5	0	14.1 ± 2.1	
Bin 6	0.1 ± 0.1	5.6 ± 1.1	
Bin 7	0	2.9 ± 0.5	
Bin 8	0	2.8 ± 0.1	
Bin 9	0	2.0 ± 0.2	
Bin 10	0	1.1 ± 0.2	
Bin 11	0	0.39 ± 0.05	
Bin 12	0	0.18 ± 0.06	

Supplementary Table 5. Bin distribution of PV-INs that innervate supragranular PNs in the SSC. Data are presented as mean ± SEM.

PV:Ai65 *SSC*	*CFP+/ H2BYFP+ Starter PNs*	*CFP+/ H2BYFP- General Inputs*	*RFP+ Input PV-INs*	*RFP+ Processes*
n = 3 animals	% of 456 cells	% of 5,077 cells	% of 665 cells	% of total RFP
L1	0	0	0	0.1 ± 0.04
L2/3	1.1 ± 0.3	4.8 ± 0.7	1.4 ± 0.8	1.7 ± 0.3
L4	8.9 ± 3.5	23.9 ± 2.0	16.4 ± 3.5	22.2 ± 2.0
L5	21.0 ± 5.5	26.6 ± 1.6	33.3 ± 4.8	26.4 ± 4.0
L6	69.0 ± 8.8	44.7 ± 2.7	48.9 ± 8.3	50.0 ± 4.1

Supplementary Table 6. Laminar distribution of PV-INs that innervate granular/infragranular PNs in the SSC. Data are presented as mean ± SEM.

PV:Ai65 *SSC*	*CFP+/ H2BYFP+ Starter PNs*	*RFP+ Input PV-INs*	*RFP+ Processes*
n = 3 animals	% of 456 cells	% of 665 cells	% of total RFP
Bin 1	0	0	0.16 ± 0.03
Bin 2	0	0	0.5 ± 0.2
Bin 3	0	0	1.2 ± 0.6
Bin 4	1.7 ± 1.0	2.9 ± 0.4	5.3 ± 1.9
Bin 5	4.4 ± 1.5	10.3 ± 3.5	12.3 ± 1.4
Bin 6	10.7 ± 2.3	11.3 ± 1.5	8.4 ± 1.7
Bin 7	9.4 ± 3.0	13.3 ± 2.9	12.0 ± 3.8
Bin 8	17.0 ± 0.4	16.0 ± 5.7	18.5 ± 4.3
Bin 9	30.4 ± 0.8	19.2 ± 1.7	19.2 ± 1.7
Bin 10	23.7 ± 5.5	10.2 ± 1.6	12.0 ± 4.8
Bin 11	2.5 ± 1.4	11.5 ± 6.6	7.3 ± 4.3
Bin 12	0.2 ± 0.2	5.4 ± 4.7	3.5 ± 3.0

Supplementary Table 7. Bin distribution of PV-INs that innervate granular/infragranular PNs in the SSC. Data are presented as mean ± SEM.

SOM-Cre:Ai65 *aSSC*	*CFP+/ H2BYFP+ Starter PNs*	*CFP+/ H2BYFP- General Inputs*	*RFP+ Input SOM-INs*	*RFP+ Processes*
n = 5 animals	% of 14,070 cells	% of 34,227 cells	% of 1,982 cells	% of total RFP
L1	0	0.1 ± 0.1	0	2.1 ± 0.3
L2/3	88.7 ± 2.9	50.9 ± 3.0	22.0 ± 3.3	39.1 ± 2.9
L4	11.3 ± 2.9	33.2 ± 2.8	32.6 ± 2.9	33.3 ± 1.4
L5	0	14.6 ± 1.1	40.6 ± 2.6	21.0 ± 1.6
L6	0	1.3 ± 0.4	4.7 ± 0.5	4.6 ± 1.0
SOM-Cre:Ai65 *MC*	*CFP+/ H2BYFP+ Starter PNs*	*CFP+/ H2BYFP- General Inputs*	*RFP+ Input SOM-INs*	*RFP+ Processes*
n = 5 animals	% of 3,370 cells	% of 10,120 cells	% of 678 cells	% of total RFP
L1	0	0	0	6.0 ± 0.7
L2/3	100 ± 0.0	80.6 ± 3.5	58.4 ± 1.6	81.0 ± 2.1
L5	0	17.6 ± 3.1	37.9 ± 1.0	11.4 ± 1.7
L6	0	1.9 ± 0.5	3.6 ± 0.7	1.7 ± 0.5

Supplementary Table 8. Laminar distribution of SOM-INs that innervate supragranular PNs in the MC and aSSC. Data are presented as mean ± SEM.

SOM-Cre:Ai65 *aSSC*	*CFP+/ H2BYFP+ Starter PNs*	*RFP+ Input SOM-INs*	*RFP+ Processes*
n = 5 animals	% of 14,070 cells	% of 1,982 cells	% of total RFP
Bin 1	0	0	3.0 ± 0.4
Bin 2	30.9 ± 10.2	3.0 ± 1.3	9.5 ± 0.5
Bin 3	50.7 ± 4.8	6.0 ± 1.8	15.8 ± 0.7
Bin 4	18.1 ± 10.6	13.2 ± 2.1	19.6 ± 1.0
Bin 5	0	14.6 ± 4.3	15.8 ± 0.8
Bin 6	0.2 ± 0.2	14.7 ± 3.3	10.3 ± 0.5
Bin 7	0	16.2 ± 2.6	8.8 ± 1.3
Bin 8	0	15.9 ± 2.0	7.9 ± 0.7
Bin 9	0	11.9 ± 2.8	5.7 ± 0.9
Bin 10	0	3.9 ± 1.3	2.2 ± 0.6
Bin 11	0	0.5 ± 0.3	0.9 ± 0.3
Bin 12	0	0	0.4 ± 0.2
SOM-Cre:Ai65 *MC*	*CFP+/ H2BYFP+ Starter PNs*	*RFP+ Input SOM-INs*	*RFP+ Processes*
n = 5 animals	% of 3,370 cells	% of 678 cells	% of total RFP
Bin 1	0.3 ± 0.2	0	5.9 ± 0.8
Bin 2	45.1 ± 7.2	6.7 ± 3.3	21.1 ± 2.9
Bin 3	47.4 ± 5.2	15.8 ± 3.5	19.8 ± 1.5
Bin 4	7.5 ± 2.9	32.8 ± 2.5	21.1 ± 2.6
Bin 5	0	20.4 ± 2.9	9.6 ± 1.3
Bin 6	0	11.1 ± 2.1	6.3 ± 1.2
Bin 7	0	9.0 ± 2.7	3.8 ± 0.7
Bin 8	0	2.5 ± 1.1	1.5 ± 0.3
Bin 9	0	1.1 ± 0.7	0.5 ± 0.1
Bin 10	0	0.2 ± 0.2	0.26 ± 0.08
Bin 11	0	0.4 ± 0.4	0.10 ± 0.05
Bin 12	0	0	0.03 ± 0.02

Supplementary Table 9. Bin distribution of SOM-INs that innervate supragranular PNs in the MC and aSSC. Data are presented as mean ± SEM.

VIP-Cre:Ai65 *SSC*	*CFP+/ H2BYFP+ Starter PNs*	*CFP+/ H2BYFP- General Inputs*	*RFP+ Input VIP-INs*	*RFP+ Processes*
n = 5 animals	% of 7,683 cells	% of 41,050 cells	% of 255 cells	% of total RFP
L1	0	0.2 ± 0.1	0	6.0 ± 0.9
L2/3	85.2 ± 5.3	48.7 ± 4.1	68.3 ± 2.2	24.4 ± 3.5
L4	14.7 ± 5.3	33.5 ± 2.8	31.3 ± 2.3	43.3 ± 2.7
L5	0.1 ± 0.1	14.7 ± 1.6	0.5 ± 0.3	19.3 ± 1.7
L6	0	3.0 ± 0.6	0	7.0 ± 0.8

Supplementary Table 10. Laminar distribution of VIP-INs that innervate supragranular PNs in the SSC. Data are presented as mean ± SEM.

VIP-Cre:Ai65 *SSC*	*CFP+/ H2BYFP+ Starter PNs*	*RFP+ Input VIP-INs*	*RFP+ Processes*
n = 5 animals	% of 7,683 cells	% of 255 cells	% of total RFP
Bin 1	0	0	7.0 ± 1.1
Bin 2	19.7 ± 3.3	12.7 ± 5.4	8.4 ± 1.4
Bin 3	57.2 ± 2.2	33.8 ± 7.6	10.9 ± 1.8
Bin 4	22.4 ± 4.7	30.9 ± 6.0	18.6 ± 1.6
Bin 5	0.7 ± 0.3	16.5 ± 2.3	17.0 ± 1.2
Bin 6	0	3.0 ± 2.2	13.0± 1.2
Bin 7	0	3.1 ± 2.0	9.2 ± 1.3
Bin 8	0	0	5.7 ± 0.2
Bin 9	0	0	4.5 ± 0.7
Bin 10	0	0	2.5 ± 0.5
Bin 11	0	0	1.9 ± 0.5
Bin 12	0	0	1.2 ± 0.4

Supplementary Table 11. Bin distribution of VIP-INs that innervate supragranular PNs in the SSC. Data are presented as mean ± SEM.